Polarization Shaping of Free-Electron Radiation by Gradient Bianisotropic Metasurfaces

Liqiao Jing, Xiao Lin, Zuojia Wang, Ido Kaminer, Hao Hu, Erping Li, Yongmin Liu, Min Chen, Baile Zhang, and Hongsheng Chen**

Free-electron radiation phenomena facilitate enticing potential to create light emission with highly tunable spectra, covering hard-to-reach frequencies ranging from microwave to X-ray. Consequently, they take part in many applications such as on-chip light sources, particle accelerators, and medical imaging. While their spectral tunability is extremely high, their polarizability is usually much harder to control. Such limitations are especially apparent in all free electron based spontaneous radiation sources, such as the Smith–Purcell (SP) radiation. Here, anomalous free-electron radiation phenomenon is demonstrated at the microwave regime from gradient bianisotropic metasurfaces, by using a phased dipole array to mimics moving charged particles. The phase gradient and the bianisotropy in metasurfaces provide new degrees of freedom for the polarization shaping of free-electron radiation, going beyond the common spectral and angular shaping. Remarkably, the observed anomalous free-electron radiation obeys a generalized SP formula derived from Fermat's principle.

1. Introduction

Free-electron radiation,[1] such as Cherenkov radiation,[2–8] transition radiation,[9–12] and Smith–Purcell (SP) radiation,[13–20] is of paramount importance to fundamental science. Free-electron radiation also enables many practical applications, including ultracompact light sources,[21–27] particle detectors,[9,28] particle accelerators,[29–31] bioimaging, and security detection.[32] Three basic and key features for free-electron radiation are the angular frequency ω (or the wavelength $\lambda = 2\pi c/\omega$), the radiation angle θ, and the polarization of emitted light (**Figure 1**), where c is the speed of light in free space. Rapid progress in the realm of free-electron radiation has fuelled a quest for the flexible shaping of all these features. Nanostructured planar lenses can provide ultrafast electromagnetic radiation with tunable illumination angle and focal length.[33] Vortex field radiation can be generated by using photon-sieve structures[34] and helical metagratings.[35] However, the very important polarization shaping for free-electron radiation[36,37] remains a long-standing challenge in experiments that is highly sought after due to its potential to enable more advanced applications. Here, we experimentally report the polarization shaping of SP radiation, along with the common spectral and angular shaping,[38] at the microwave regime by using a gradient bianisotropic metasurface (Figure 1).

Ever since the first observation in 1953,[13] SP radiation has become a well-known phenomenon of free-electron radiation. It has the capability of generating light in such frequency ranges as

Dr. L. Jing, Dr. X. Lin, Prof. Z. Wang, Prof. H. Chen
Interdisciplinary Center for Quantum Information, State Key Laboratory of Modern Optical Instrumentation, College of Information Science and Electronic Engineering
Zhejiang University
Hangzhou 310027, China
E-mail: zuojiawang@zju.edu.cn; hansomchen@zju.edu.cn

Dr. L. Jing, Prof. M. Chen
Department of Physics
Massachusetts Institute of Technology
Cambridge, MA 02139, USA

Dr. L. Jing, Dr. X. Lin, Prof. Z. Wang, Prof. E. Li, Prof. H. Chen
International Joint Innovation Center, ZJU-UIUC Institute
The Electromagnetic Academy at Zhejiang University
Zhejiang University
Haining 314400, China

The ORCID identification number(s) for the author(s) of this article can be found under https://doi.org/10.1002/lpor.202000426

DOI: 10.1002/lpor.202000426

Prof. I. Kaminer
Department of Electrical Engineering
Technion – Israel Institute of Technology
Haifa 32000, Israel

Dr. H. Hu
School of Electrical and Electronic Engineering
Nanyang Technological University
Nanyang Avenue, Singapore 639798, Singapore

Y. Liu
Departments of Mechanical and Industrial Engineering and Electrical and Computer Engineering
Northeastern University
Boston, MA 02115, USA

Prof. B. Zhang
Division of Physics and Applied Physics, School of Physical and Mathematical Sciences
Nanyang Technological University
21 Nanyang Link, Singapore 637371, Singapore

Prof. B. Zhang
Centre for Disruptive Photonic Technologies
Nanyang Technological University
Singapore 637371, Singapore

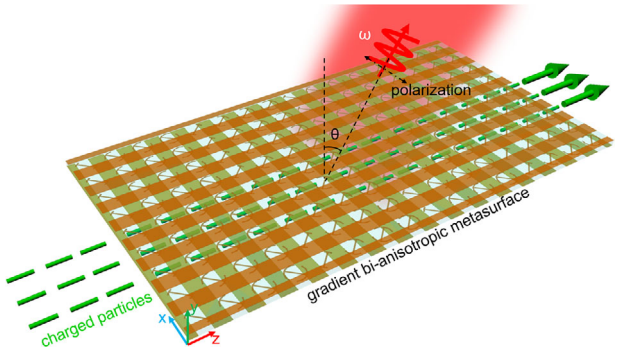

Figure 1. Schematic of the polarization, angular, and spectral shaping of free-electron radiation from gradient bianisotropic metasurfaces. Here and below, a uniform sheet of electrons moves with a velocity $\bar{v} = \hat{z}\, v$ along a trajectory parallel to the metasurface plane, where $v = 0.35c$. The radiation angle θ is the angle between the y axis and the wavevector of emitted light.

terahertz, deep ultraviolet, and X-ray,[18,23,39] which are difficult to reach through other technologies. Consider a swift electron moves with the velocity $\bar{v} = \hat{z}\, v$ along a trajectory parallel to the surface of periodic structures (e.g., the grating) with a pitch p; the conventional SP radiation is governed by the celebrated SP formula,[13] that is,

$$\sin\theta = \frac{c}{v} - m\frac{\lambda}{p} \tag{1}$$

where m is the integer diffraction order, λ is the wavelength of radiated waves. The SP formula has been well tested in numerous experiments and provided useful guidance for on-demand design of tunable radiation and various applications.[16,17,32,35,38,40–43] On the other hand, it is recently theoretically shown that the advent of gradient metasurfaces[44–48] provides new degrees of freedom for the manipulation of free-electron radiation.[49] For example, if we introduce the phase gradient or phase discontinuity into the periodic structure (i.e., the gradient metasurface), Equation (1) can be generalized into

$$\sin\theta = \frac{c}{v} - m\frac{\lambda}{p} + \frac{\lambda}{2\pi}\cdot\frac{d\varphi}{dz} \tag{2}$$

where $\frac{d\varphi}{dz}$ is the phase gradient along electron's propagation direction. Note that the reflection and refraction from gradient metasurfaces follows the generalized diffraction laws derived from Fermat's principle (i.e., the trajectory between two points taken by a ray of light is that of the least optical path);[46] such exotic phenomena are denoted as the anomalous reflection and refraction in the literature.[44–46] By following such terminology, Equation (2) is denoted as the generalized SP formula. However, the experimental confirmation of the generalized SP formula remains seldom explored, despite the intriguing potential of gradient metasurfaces in shaping the light emission.

Here, we experimentally observe the anomalous free-electron radiation phenomenon from gradient bianisotropic metasurfaces. The excellent agreement between our experimental and theoretical results successfully verifies that the observed anomalous radiation phenomenon obeys the generalized SP formula,

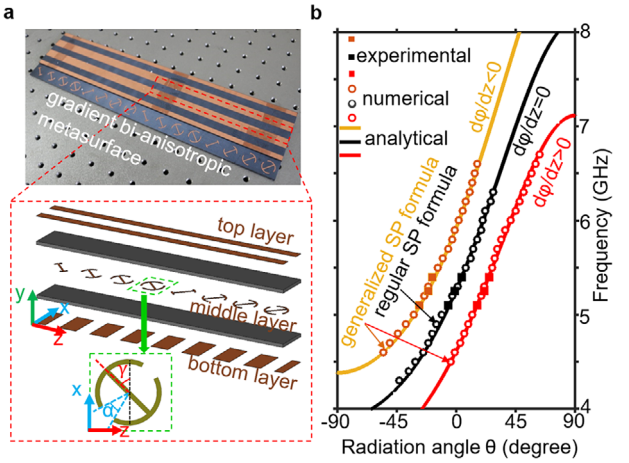

Figure 2. Experimental, numerical, and analytical study of the anomalous free-electron radiation phenomenon obeying the generalized Smith–Purcell (SP) formula. a) Experimental sample of the gradient bianisotropic metasurface (top panel), along with the structural schematic of its super cell consisting of eight unit cells (bottom panel). In each unit cell of the middle layer, the symmetric split ring has an open angle α, and the central line of the opening (red dashed line) is azimuthally rotated by an angle γ with respect to the x axis. b) Radiation angle θ as a function of the frequency $\omega/2\pi$ at three typical phase gradients $d\varphi/dz$, namely $d\varphi/dz \cdot p = \pm\pi/4$ or 0, where p is the pitch of metasurface. The analytical lines are calculated according to either the regular SP formula in Equation (1) or the generalized SP formula in Equation (2), where the diffraction order is $m = -1$; the numerical data are extracted from the CST simulation; the experimental data are extracted from Figure 4. The phase gradient provides an extra degree of freedom for the spectral and angular shaping of emitted light.

instead of the regular SP formula, if the phase gradient is nonzero (**Figure 2**). The phase gradient in the generalized SP formula thus provides an extra degree of freedom to facilitate the spectral and angular shaping of free-electron radiation. Moreover, while both Equations (1 and 2) only describe the relation between the radiation angle and the frequency of emitted light, we find that the bianisotropy in gradient bianisotropic metasurfaces can also provide an extra degree of freedom to facilitate the polarization shaping. Therefore, our work indicates that the gradient bianisotropic metasurface can provide a promising powerful platform for the flexible control of free-electron radiation.

2. Results

The anomalous free-electron radiation from a gradient bianisotropic metasurface is schematically shown in Figure 1. Consider a uniform sheet of moving electrons; the induced current density in the time domain is $\bar{J}(\bar{r},t) = \hat{z}\, qv\delta(y-y_0)\delta(z-vt)$,[9,10] where q is the charge. After the Fourier transformation, the induced current density in the frequency domain can be expressed as $\bar{J}(\bar{r},\omega) = \frac{1}{2\pi}\int \bar{J}(\bar{r},t)e^{i\omega t}dt = \hat{z}\,\frac{qv}{2\pi}\delta(y-y_0)e^{ik_z z}$, where $k_z = \omega/v$.[9,10] Such a form of current density in the frequency domain can be effectively mimicked by the phased dipole array (Figures S1–S3, Supporting Information), which can be further effectively generated for example by the slot waveguide, as verified[9]. On the other hand, the radiated power from electrons at the microwave frequency is generally small. To facilitate the

experimental observation of the anomalous radiation phenomenon, the slot waveguide is used to imitate the moving electron sheet in the microwave experiments, while the realistic moving electron sheet is used in the analytical calculation and numerical simulation.

Figure 2a schematically shows the structure of gradient bianisotropic metasurfaces used in the experiment. To be specific, the gradient bianisotropic metasurface has a pitch $p = 20$ mm and consists of three metallic layers. The three metallic layers are separated by two F4B dielectric slabs. For each dielectric slab, it has a thickness of 4 mm and a relative permittivity of $\varepsilon_r = 2.65 + 0.01\mathrm{i}$. For metal, the copper with a conductivity $\sigma = 5.8 \times 10^7$ S/m and a thickness of 0.035 mm is adopted. Both the top and bottom layers are one-dimensional (1D) metallic gratings. These two sets of gratings are orthogonal to each other, and the neighboring metal strips are separated by an air gap of 9 mm. We add the phase gradient and the bianisotropy in the middle layer, whose super- cell consists of eight unit cells (Figure S4, Supporting Information). Each unit cell is composed of a symmetric split ring resonator connected by a cut wire, where α represents the open angle of the symmetric split ring and γ is the azimuthal rotation angle of unit cell. Accordingly, the arbitrary phase gradient in the middle layer can be effectively constructed by gradually varying the values of α and/or γ (Figure S5, Supporting Information).

We now proceed to the verification of the generalized SP formula, by directly comparing the analytically, numerically, and experimentally obtained relations of the radiation angle and the frequency in Figure 2b. Within the studied frequency range in Figure 2b, the moving electron has a velocity $v = 0.35c$, and its trajectory is 0.5 mm beneath the metasurface plane. Without loss of generality, the analytical, numerical, and experimental results are given at three typical phase gradients of the metasurface, namely $\frac{d\varphi}{dz} \cdot p = 0$ or $\pm\frac{\pi}{4}$. For the cases with $\frac{d\varphi}{dz} \cdot p = 0$ and $\frac{d\varphi}{dz} \cdot p \neq 0$, the analytical results are calculated according to the regular SP formula in Equation (1) and the generalized SP formula in Equation (2), respectively. For conceptual demonstration, only the diffraction order $m = -1$ in Equations (1 and 2) is considered. Numerical data are extracted from the field distribution of emitted light via the particle-in-cell simulation through the commercial software CST (**Figure 3**a-c and Figure S6, Supporting Information), by using a finite-size electron sheet. Experimental data are extracted from the field distribution on top of a slot waveguide via microwave measurements. All cases in Figure 2b show the excellent agreement between the experimental, numerical, and analytical results. Importantly, Figure 2b shows that if $\frac{d\varphi}{dz} \cdot p \neq 0$, the SP radiation would not obey the regular SP formula but is governed by the generalized SP formula.

Figure 3 numerically shows the field distribution of emitted light at 5.25 GHz, where the field propagation direction is governed by the generalized SP formula. In order to clearly demonstrate the influence of phase gradient on the light emission, we set the pitch of metasurface to be $p = -m\nu\lambda/c$ at 5.25 GHz, where $m = -1$. This way, Equation (2) is simplified to $\sin\theta = \frac{\lambda}{2\pi} \cdot \frac{d\varphi}{dz}$. That is, if $\frac{d\varphi}{dz} = 0$, the propagation direction of emitted light would be perpendicular to the metasurface plane (Figure 3b). If $\frac{d\varphi}{dz} > 0$, the emitted light propagates to the $+\hat{z}$ direction (e.g., $\frac{d\varphi}{dz} \cdot p = +\frac{\pi}{4}$ in Figure 3a). In contrast, if $\frac{d\varphi}{dz} < 0$, the propagation direction of emitted light becomes to the $-\hat{z}$ direction (e.g., $\frac{d\varphi}{dz} \cdot p = -\frac{\pi}{4}$ in Figure 3c).

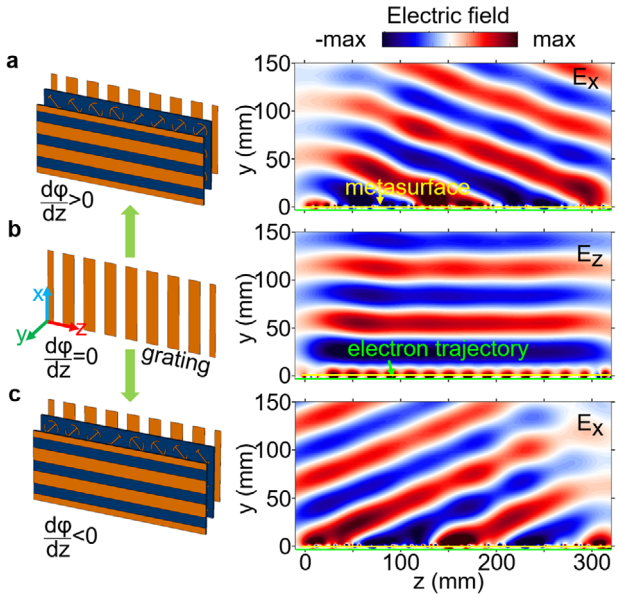

Figure 3. Numerical simulation of the anomalous free-electron radiation phenomenon at 5.25 GHz. The trajectory of the electron sheet (green line in each panel) is 0.5 mm beneath the metasurface plane (yellow line). a) Gradient bianisotropic metasurface with $d\varphi/dz \cdot p = +\pi/4$. b) Metasurface without gradient and bianisotropy, namely the grating. c) Gradient bianisotropic metasurface with $d\varphi/dz \cdot p = -\pi/4$. The simultaneous existence of phase gradient and bianisotropy in the metasurface provide extra degrees of freedom for the polarization, spectral, and angular shaping of free-electron radiation.

Moreover, Figure 3 numerically shows the polarization of emitted light can be modulated by the gradient bianisotropic metasurface. For the case of $\frac{d\varphi}{dz} = 0$, one may use the three-layered metasurface by setting its middle layer to have 8 same unit cells in the super cell. Alternatively, one can directly use the 1D metallic grating (e.g., the bottom layer of the three-layered metasurface) for simplicity (Figure 3b). For the grating (or periodic direction) along the z direction, the conventional SP radiation has its electric field always polarized along the z direction (Figures 3b and Figure S7, Supporting Information). The underlying mechanism is that the spatially extended interaction between moving electrons and the grating along the z direction can effectively create a bunch of electric dipoles only oscillating along the z direction.

In contrast, for the cases of $\frac{d\varphi}{dz} \neq 0$, the anomalous SP radiation has the electric field mainly polarized along the x direction (Figure 3a,c) and Figure S7, Supporting Information). In other words, the polarizations of emitted light in Figure 3a,b,c are almost perpendicular to each other. Such an exotic polarization shaping phenomenon of emitted light is enabled by the bianisotropy in the middle layer of the designed three-layered metasurface. That is, the bianisotropic middle layer can efficiently transform the emitted E_z fields from the bottom layer to their cross-polarized ones (i.e., E_x), when the emitted light passes through the middle layer. We highlight that the top or bottom grating layer is specially designed to behave like a non-perfect polarization filter within the studied frequency range (Figure S8, Supporting Information). In other words, the two perpendicular

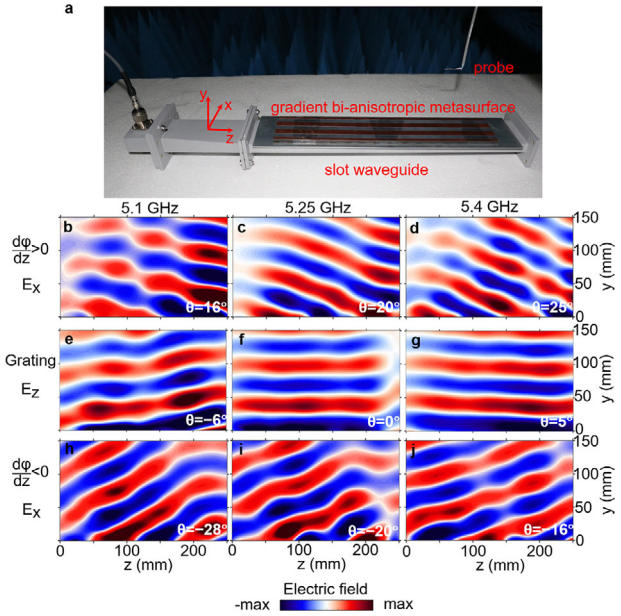

Figure 4. Experimental observation of the anomalous free-electron radiation phenomenon. a) Experimental measurement setup (Figure S9, Supporting Information). In the microwave experiment, a slot waveguide is used to effectively generate the phased dipole array, which can mimic the evanescent fields carried by the electrons moving along the $+\hat{z}$ direction at the studied frequency (Figures S1–S3, Supporting Information). b–j) Measured field distributions of emitted light in the yz plane. The metasurface is located at the $y = 0$ plane. The working frequency is 5.1 GHz in (b,e,h), 5.25 GHz in (c,f,i), and 5.4 GHz in (d,g,j). The phase gradient is $d\varphi/dz \cdot p = +\pi/4$ in (b–d), $d\varphi/dz \cdot p = 0$ in (e–g), and $d\varphi/dz \cdot p = -\pi/4$ in (h–j). The measured electric field of emitted light is mainly polarized along the x direction in (b–d, h–j), while it is polarized along the z direction in (e–g).

gratings cannot induce the polarization shaping. As a clear evidence, if the middle layer in Figure 3a,c is removed, the emitted light in the $y > 0$ region would possess the negligible E_x field (but weak E_z field) (Figure S8, Supporting Information), due to the negligible coupling of cross-polarized light between the two perpendicular metallic gratings. Therefore, the middle layer with the phase gradient and the bianisotropy plays a key role in the polarization shaping of emitted light, besides the spectral and angular shaping.

Figure 4 shows the experimental observation of the anomalous SP radiation. The experimental measurement setup is shown in Figure 4a and Figure S9 (Supporting Information). In the microwave experiment, the slot waveguide is placed 0.5 mm beneath the bottom layer of metasurface. Due to the advanced microwave technology, the amplitude and phase of emitted light can be simultaneously measured by using the near-field scanning platform in an anechoic chamber.[50,51] In Figure 4b-j, three typical metasurfaces with the phase gradient $\frac{d\varphi}{dz} \cdot p = 0$ or $\pm \frac{\pi}{4}$ are experimentally tested at three different frequencies, namely 5.1, 5.25, and 5.4 GHz.

Regarding the spectral and angular shaping of emitted light, the radiation angle is changed from 16°, −6° to −28° at 5.1 GHz in Figure 4b,e,h, from 20°, 0° to −20° at 5.25 GHz in Figure 4c,f,i, and from 25°, 5° to −16° at 5.4 GHz in Figure 4d,g,j, if the phase gradient $\frac{d\varphi}{dz} \cdot p$ in the metasurface varies from $+\frac{\pi}{4}$, 0 to $-\frac{\pi}{4}$. To facilitate the direct comparison, the relation of the radiation angle and the frequency is extracted from the measurement in Figure 4b-j and added in Figure 2b. From Figure 2b, these measured results are in very good agreement with the theoretical prediction. As such, our microwave observation successfully proves the validity of the generalized SP formula.

Regarding the polarization shaping of emitted light, the measured electric field is polarized along the z direction if the 1D grating is used (Figure 4e-g), and it would be dominantly polarized along the x direction if the gradient bianisotropic metasurface is used (Figure 4b-d, h-j). These measured results are in very good agreement with the simulation results in Figure 3 and Figure S6, Supporting Information. Our experiment thus proves the capability of gradient bianisotropic metasurfaces in the polarization shaping of free-electron radiation. Note that the phase gradient is not a necessary condition to realize the polarization shaping.[36]

3. Conclusion

In conclusion, we have observed the anomalous free-electron radiation phenomenon, which obeys the generalized SP formula derived from Fermat's principle, from gradient bianisotropic metasurfaces. Moreover, we have experimentally observed the polarization shaping of free-electron radiation using gradient bianisotropic metasurfaces, along with the angular and spectra shaping. The polarization shaping of light emission goes beyond the description of the generalized SP formula. The revealed technique for the flexible shaping of free-electron radiation should be applicable in other frequencies ranging from terahertz to ultraviolet. Therefore, our work further indicates that the gradient bianisotropic metasurface can provide a promising versatile platform for the flexible manipulation of free-electron radiation and may boost the development of future on-chip nanophotonic circuits and devices, such as on-chip free-electron light sources (with controllable polarization, frequency, and propagation direction), as well as miniaturized particle accelerators, and novel sensing and diagnostic devices.

4. Experimental Section

Numerical Simulation: The particle-in-cell studio in the commercial software CST was used for the numerical simulation of SP radiation in this work. Acceleration voltage was 35 kV and 0.5 A sheet electron beam was used in the simulation. The cross-section of the electron sheet was 60 × 0.5 mm, the rise time was 0.1 ns, and the electron velocity was $v = 0.35c$. In order to accelerate the numerical simulation and save the CPU memory, the designed metasurface was composed of 3 × 16 unit cells along x and z directions, respectively. The boundary conditions at x, y, and z directions were all set to be open boundary conditions. The distance between the electron trajectory and the metasurface plane was 0.5 mm. An external magnetic field with $B_z = 1$ Tesla was applied to spatially bound the electron beam so that the electron beam would move straightforward along the z direction.

Experimental Apparatus and Setup: The detailed measurement setup is shown in Figure S9 (Supporting Information). In the microwave experiment, an Agilent network analyzer and a two-dimensional near-field scanning platform were employed. The constructed slot waveguide in Figure 4a was built by the aluminum and had a dimensions of 60 ×12 × 400 mm; its slot size was 60 × 2 mm. The transverse electric (TE) mode in the slot

waveguide (Figure S2, Supporting Information) was used to effectively generate the phased dipole array, which could further mimic the evanescent fields carried by the moving electrons at the studied frequency. An additional gradient waveguide was added at the input-port side of the slot waveguide (or left side in Figure 4a) so that the TE_{10} mode in the slot waveguide could be selectively and efficiently excited. To be specific, for the gradient regular–regular waveguide transducer (Figure S3, Supporting Information), its input port was judiciously designed to only support the TE_{10} mode within our studied frequency range; moreover, both its width and height were gradually varied along the *z* direction, so that the excited TE_{10} mode at the input port of the gradient waveguide could be efficiently transformed into the TE_{10} mode inside the slot waveguide. The gradient bianisotropic metasurfaces had a dimension of $60 \times 4.105 \times 320$ mm, and they were fabricated using the PCB technology (Figure 4a).

Supporting Information

Supporting Information is available from the Wiley Online Library or from the author.

Conflict of Interest

The authors declare no conflict of interest.

Acknowledgements

L.J. and X.L. contributed equally to this work. The work at Zhejiang University was sponsored by the National Natural Science Foundation of China (6180128, 61625502, 11961141010, and 61975176), the Top-Notch Young Talents Program of China, and the Fundamental Research Funds for the Central Universities.

Keywords

bianisotropy, free-electron radiation, gradient metasurfaces, polarization shaping

Received: September 28, 2020
Revised: December 15, 2020
Published online: February 25, 2021

[1] F. G. De Abajo, *Rev. Mod. Phys.* **2010**, *82*, 209.
[2] P. Cherenkov, *Science* **1960**, *131*, 136.
[3] H. Chen, M. Chen, *Mater. Today* **2011**, *14*, 34.
[4] P. Genevet, D. Wintz, A. Ambrosio, A. She, R. Blanchard, F. Capasso, *Nat. Nanotechnol.* **2015**, *10*, 804.
[5] X. Shi, X. Lin, F. Gao, H. Xu, Z. Yang, B. Zhang, *Phys. Rev. B* **2015**, *92*, 081404.
[6] Z. Duan, X. Tang, Z. Wang, Y. Zhang, X. Chen, M. Chen, Y. Gong, *Nat. Commun.* **2017**, *8*, 14901.
[7] C. Luo, M. Ibanescu, S. G. Johnson, J. Joannopoulos, *Science* **2003**, *299*, 368.
[8] S. Xi, H. Chen, T. Jiang, L. Ran, J. Huangfu, B.-I. Wu, J. A. Kong, M. Chen, *Phys. Rev. Lett.* **2009**, *103*, 194801.
[9] X. Lin, S. Easo, Y. Shen, H. Chen, B. Zhang, J. D. Joannopoulos, M. Soljačić, I. Kaminer, *Nat. Phys.* **2018**, *14*, 816.
[10] X. Lin, I. Kaminer, X. Shi, F. Gao, Z. Yang, Z. Gao, H. Buljan, J. D. Joannopoulos, M. Soljačić, H. Chen, *Sci. Adv.* **2017**, *3*, e1601192.
[11] V. L. Ginzburg, V. N. Tsytovich, *Transition Radiation and Transition Scattering*CRC Press, Boca Raton, FL **1990**.
[12] B. Dolgoshein, *Nucl. Instrum. Methods Phys. Res., Sect. A* **1993**, *326*, 434.
[13] S. J. Smith, E. Purcell, *Phys. Rev.* **1953**, *92*, 1069.
[14] I. Kaminer, S. Kooi, R. Shiloh, B. Zhen, Y. Shen, J. López, R. Remez, S. Skirlo, Y. Yang, J. Joannopoulos, *Phys. Rev. X* **2017**, *7*, 011003.
[15] Y. Yang, A. Massuda, C. Roques-Carmes, S. E. Kooi, T. Christensen, S. G. Johnson, J. D. Joannopoulos, O. D. Miller, I. Kaminer, M. Soljačić, *Nat. Phys.* **2018**, *14*, 894.
[16] A. Massuda, C. Roques-Carmes, Y. Yang, S. E. Kooi, Y. Yang, C. Murdia, K. K. Berggren, I. Kaminer, M. Soljačic´, *ACS Photonics* **2018**, *5*, 3513.
[17] J. Gardelle, P. Modin, J. Donohue, *Phys. Rev. Lett.* **2010**, *105*, 224801.
[18] S. Korbly, A. Kesar, J. Sirigiri, R. Temkin, *Phys. Rev. Lett.* **2005**, *94*, 054803.
[19] J.-K. So, F. J. García de Abajo, K. F. MacDonald, N. I. Zheludev, *ACS Photonics* **2015**, *2*, 1236.
[20] J. Saavedra, D. Castells-Graells, F. J. G. de Abajo, *Phys. Rev. B* **2016**, *94*, 035418.
[21] G. Adamo, K. F. MacDonald, Y. Fu, C. Wang, D. Tsai, F. G. de Abajo, N. Zheludev, *Phys. Rev. Lett.* **2009**, *103*, 113901.
[22] F. Liu, L. Xiao, Y. Ye, M. Wang, K. Cui, X. Feng, W. Zhang, Y. Huang, *Nat. Photonics* **2017**, *11*, 289.
[23] Y. Ye, F. Liu, M. Wang, L. Tai, K. Cui, X. Feng, W. Zhang, Y. Huang, *Optica* **2019**, *6*, 592.
[24] C. Roques-Carmes, S. E. Kooi, Y. Yang, A. Massuda, P. D. Keathley, A. Zaidi, Y. Yang, J. D. Joannopoulos, K. K. Berggren, I. Kaminer, *Nat. Commun.* **2019**, *10*, 3176.
[25] G. Adamo, J.-Y. Ou, J. So, S. Jenkins, F. De Angelis, K. F. MacDonald, E. Di Fabrizio, J. Ruostekoski, N. I. Zheludev, *Phys. Rev. Lett.* **2012**, *109*, 217401.
[26] S. Liu, P. Zhang, W. Liu, S. Gong, R. Zhong, Y. Zhang, M. Hu, *Phys. Rev. Lett.* **2012**, *109*, 153902.
[27] L. J. Wong, I. Kaminer, O. Ilic, J. D. Joannopoulos, M. Soljačić, *Nat. Photonics* **2016**, *10*, 46.
[28] V. Ginis, J. Danckaert, I. Veretennicoff, P. Tassin, *Phys. Rev. Lett.* **2014**, *113*, 167402.
[29] E. Peralta, K. Soong, R. England, E. Colby, Z. Wu, B. Montazeri, C. McGuinness, J. McNeur, K. Leedle, D. Walz, *Nature* **2013**, *503*, 91.
[30] K. Mizuno, S. Ono, O. Shimoe, *Nature* **1975**, *253*, 184.
[31] K. Mizuno, J. Pae, T. Nozokido, K. Furuya, *Nature* **1987**, *328*, 45.
[32] T. M. Shaffer, E. C. Pratt, J. Grimm, *Nat. Nanotechnol.* **2017**, *12*, 106.
[33] N. Talebi, S. Meuret, S. Guo, M. Hentschel, A. Polman, H. Giessen, P. A. van Aken, *Nat. Commun.* **2019**, *10*, 599.
[34] N. van Nielen, M. Hentschel, N. Schilder, H. Giessen, A. Polman, N. Talebi, *Nano Lett.* **2020**, *20*, 5975.
[35] L. Jing, Z. Wang, X. Lin, B. Zheng, S. Xu, L. Shen, Y. Yang, F. Gao, M. Chen, H. Chen, *Research* **2019**, *2019*, 3806132.
[36] Z. Wang, K. Yao, M. Chen, H. Chen, Y. Liu, *Phys. Rev. Lett.* **2016**, *117*, 157401.
[37] Y. Yang, C. Roques-Carmes, I. Kaminer, A. Zaidi, A. Massuda, Y. Yang, S. E. Kooi, K. Berggren, M. Soljačić, presented at Conf. on Lasers and Electro-Optics **2018**.
[38] R. Remez, N. Shapira, C. Roques-Carmes, R. Tirole, Y. Yang, Y. Lereah, M. Soljačić, I. Kaminer, A. Arie, *Phys. Rev. A* **2017**, *96*, 061801.
[39] M. J. Moran, *Phys. Rev. Lett.* **1992**, *69*, 2523.
[40] G. Doucas, J. Mulvey, M. Omori, J. Walsh, M. Kimmitt, *Phys. Rev. Lett.* **1992**, *69*, 1761.
[41] K. Woods, J. Walsh, R. Stoner, H. Kirk, R. Fernow, *Phys. Rev. Lett.* **1995**, *74*, 3808.
[42] J. Urata, M. Goldstein, M. Kimmitt, A. Naumov, C. Platt, J. Walsh, *Phys. Rev. Lett.* **1998**, *80*, 516.
[43] L. Comandar, B. Fröhlich, M. Lucamarini, K. Patel, A. Sharpe, J. Dynes, Z. Yuan, R. Penty, A. Shields, *Appl. Phys. Lett.* **2014**, *104*, 021101.
[44] N. Yu, F. Capasso, *Nat. Mater.* **2014**, *13*, 139.

[45] A. V. Kildishev, A. Boltasseva, V. M. Shalaev, *Science* **2013**, *339*, 1232009.
[46] N. Yu, P. Genevet, M. A. Kats, F. Aieta, J.-P. Tetienne, F. Capasso, Z. Gaburro, *Science* **2011**, *334*, 333.
[47] S. Sun, K.-Y. Yang, C.-M. Wang, T.-K. Juan, W. T. Chen, C. Y. Liao, Q. He, S. Xiao, W.-T. Kung, G.-Y. Guo, *Nano Lett.* **2012**, *12*, 6223.
[48] S. Sun, Q. He, S. Xiao, Q. Xu, X. Li, L. Zhou, *Nat. Mater.* **2012**, *11*, 426.
[49] Z. Su, F. Cheng, L. Li, Y. Liu, *ACS Photonics* **2019**, *6*, 1947.
[50] C. Qian, X. Lin, Y. Yang, X. Xiong, H. Wang, E. Li, I. Kaminer, B. Zhang, H. Chen, *Phys. Rev. Lett.* **2019**, *122*, 063901.
[51] L. Jing, Z. Wang, R. Maturi, B. Zheng, H. Wang, Y. Yang, L. Shen, R. Hao, W. Yin, E. Li, *Laser Photonics Rev.* **2017**, *11*, 1700115.